Electronic Supplementary Information

Energy transfer between rare earths in layered rare-earth hydroxides

Pingping Feng, Xinying Wang, Yushuang Zhao, De-Cai Fang, Xiaojing Yang*

College of Chemistry, Beijing Normal University, Beijing, 100875, China. E-mail: yang.xiaojing@bnu.edu.cn; Fax: +86-10-5880-2075; Tel: +86-10-5880-2960.

The abbreviations of the reliability factors (*R*-factors) and goodness-of-fit indicator after the Rietveld refinement.

R_{wp}: weighted pattern *R*-factor

R_p: pattern *R*-factor

R_R: Rietveld *R*-factor

R_e: Expected *R*-factor

S: Goodness-of-fit indicator

SEM/EDX: scanning electron microscopy/energy-dispersive x-ray analysis (FESEM, S-8010, Hitachi; EDX, XFlash6160, BRUKER)

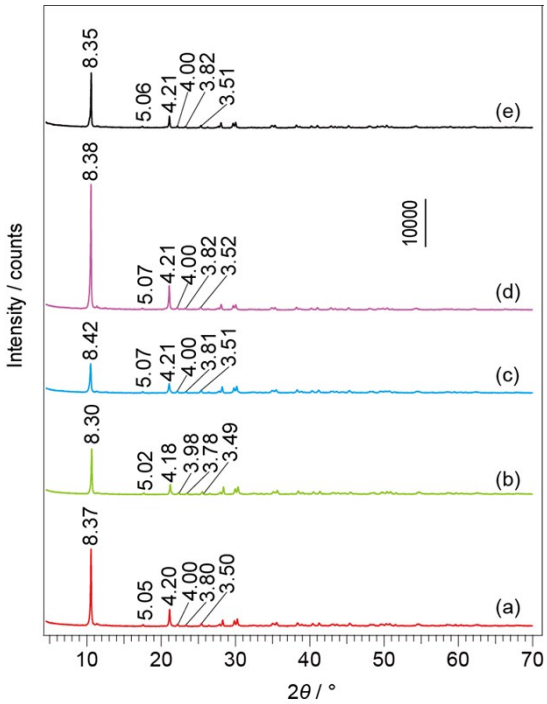

Fig. S1 XRD patterns for Cl^{-}-$LEu_xTb_{1-x}Hs$ of (a) x = 0, (b) x = 0.05, (c) x = 0.2, (d) x = 0.8 and (e) x=0.95.

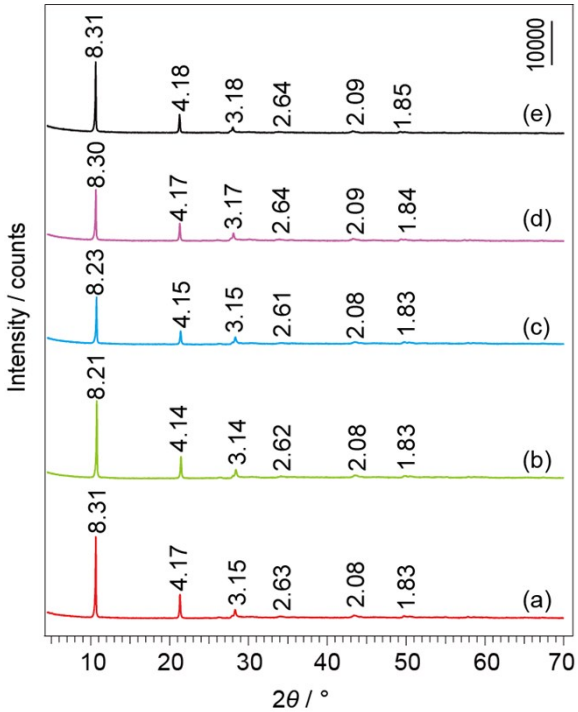

Fig. S2 XRD patterns for NO_3^{-}-$LEu_xTb_{1-x}Hs$ of (a) x = 0, (b) x = 0.05, (c) x = 0.2, (d) x = 0.8 and (e) x=0.95.

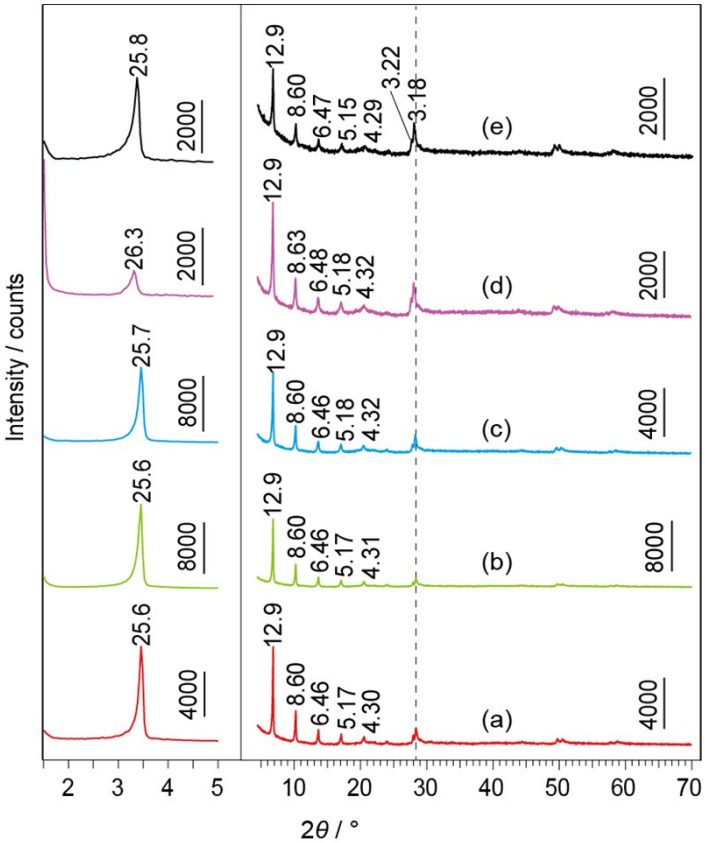

Fig. S3 XRD patterns for DS^{-}-$LEu_xTb_{1-x}Hs$ of (a) x = 0, (b) x = 0.05, (c) x = 0.2, (d) x = 0.8 and (e) x=0.95.

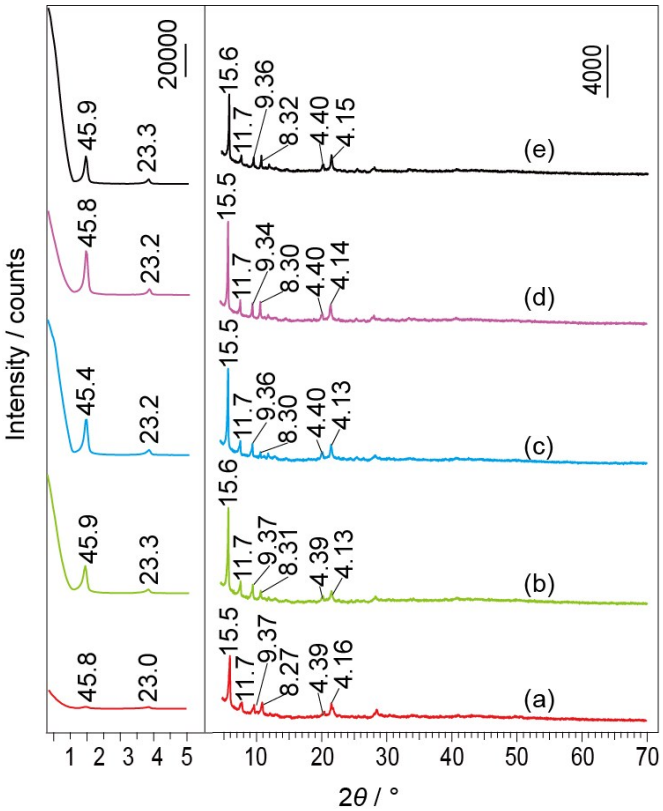

Fig. S4 XRD patterns for OA^--$LEu_xTb_{1-x}Hs$ of (a) x = 0, (b) x = 0.05, (c) x = 0.2, (d) x = 0.8 and (e) x=0.95.

Table S1 Basal Spacing of the Various $LEu_xTb_{1-x}H$ Samples.

x	d_{basal} / Å				
	Cl^-	NO_3^-	DS^-	OA^-	NSs
0	8.37	8.31[*1]	27.2	45.8	∞[*2]
0.05	8.30	8.21	26.7	45.9	∞
0.2	8.42	8.23	26.2	45.4	∞
0.5	8.32	8.31	25.3	45.9	∞
0.8	8.38	8.30	26.2	45.8	∞
0.95	8.35	8.31	26.2	45.9	∞

[*1] NO_3^--LTbH with the d_{basal} of 8.21 Å was also obtained.

[*2]No peaks but halo was observed in the XRD patterns for the delaminated samples. ∞ is used here, but we consider that the inclusion volume effect in liquid crystal should take place, the distance between the 2 dimensional crystals depends on the volume of the delamination formamide.

Table S2 Chemical analysis results for the series samples of Cl^--$LEu_xTb_{1-x}Hs$.

Designed x	Content calculated (found) (wt %)					Chemical formula
	Eu	Tb	Cl	C	H	
0.05	3.12 (3.33)	58.74 (62.77)	6.15 (6.57)	0.33 (0.35)	1.82 (1.95)	$Eu_{0.05}Tb_{0.95}(OH)_{2.42}Cl_{0.44}(CO_3)_{0.07}\cdot1.13H_2O$
0.2	11.75 (12.65)	50.30 (54.14)	5.73 (6.16)	0.29 (0.31)	1.77 (1.90)	$Eu_{0.20}Tb_{0.80}(OH)_{2.47}Cl_{0.41}(CO_3)_{0.06}\cdot1.01H_2O$
0.5	31.96 (33.41)	32.29 (33.74)	6.19 (6.47)	0.31 (0.32)	1.73 (1.81)	$Eu_{0.51}Tb_{0.49}(OH)_{2.45}Cl_{0.42}(CO_3)_{0.06}\cdot0.87H_2O$
0.8	52.57 (53.06)	13.60 (13.73)	6.50 (6.57)	0.31 (0.31)	1.82 (1.84)	$Eu_{0.80}Tb_{0.20}(OH)_{2.46}Cl_{0.42}(CO_3)_{0.06}\cdot0.88H_2O$
0.95	61.43 (62.75)	3.47 (3.54)	6.33 (6.47)	0.35 (0.34)	1.89 (1.85)	$Eu_{0.95}Tb_{0.05}(OH)_{2.45}Cl_{0.42}(CO_3)_{0.07}\cdot0.94H_2O$

Table S3 Chemical analysis results for the series samples of NO_3^--$LEu_xTb_{1-x}Hs$.

Designed x	Content found (calculated) (wt %)					Chemical formula
	Eu	Tb	C	H	N	
0	—	58.6 (62.7)	0.64 (0.66)	1.59 (1.71)	2.45 (2.60)	$Tb(OH)_{2.24}(NO_3)_{0.47}(CO_3)_{0.14}\cdot1.05H_2O$
0.05	2.82 (2.60)	61.8 (57.07)	0.57 (0.53)	1.78 (1.64)	1.94 (1.79)	$Eu_{0.05}Tb_{0.95}(OH)_{2.42}(NO_3)_{0.34}(CO_3)_{0.12}\cdot0.97H_2O$
0.2	10.71 (11.73)	47.65 (52.17)	0.62 (0.68)	1.71 (1.87)	1.66 (1.82)	$Eu_{0.19}Tb_{0.81}(OH)_{2.40}(NO_3)_{0.32}(CO_3)_{0.14}\cdot1.11H_2O$
0.5	29.68 (31.86)	31.28 (33.57)	0.63 (0.68)	1.58 (1.70)	1.62 (1.74)	$Eu_{0.50}Tb_{0.50}(OH)_{2.44}(NO_3)_{0.32}(CO_3)_{0.13}\cdot0.80H_2O$

0.8	46.40 (48.92)	12.81 (13.51)	0.50 (0.56)	1.65 (1.85)	2. 08 (2.35)	$Eu_{0.79}Tb_{0.21}(OH)_{2.36}(NO_3)_{0.41}(CO_3)_{0.12}\cdot 1.10H_2O$
0.95	58.95 (62.38)	3.30 (3.49)	0.66 (0.65)	1.65 (1.63)	1.75 (1.73)	$Eu_{0.95}Tb_{0.05}(OH)_{2.46}(NO_3)_{0.29}(CO_3)_{0.13}\cdot 0.66H_2O$

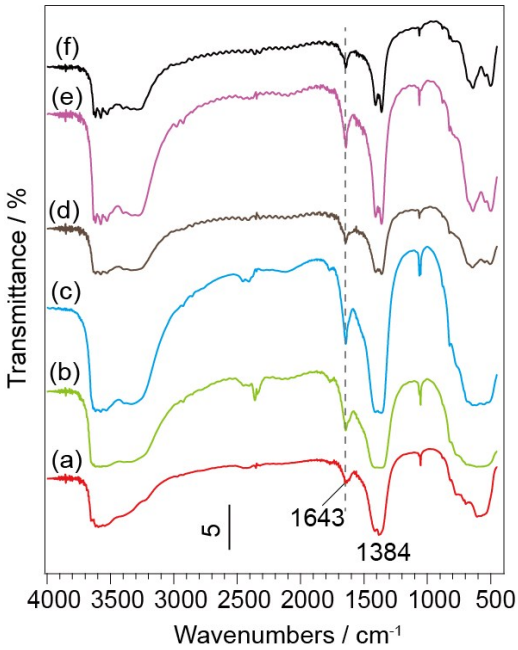

Fig. S5 FT-IR spectra for NO_3^--$LEu_xTb_{1-x}Hs$ of (a) x = 0, (b) x = 0.05, (c) x = 0.2, (d) x = 0.5, (e) x = 0.8 and (f) x=0.95.

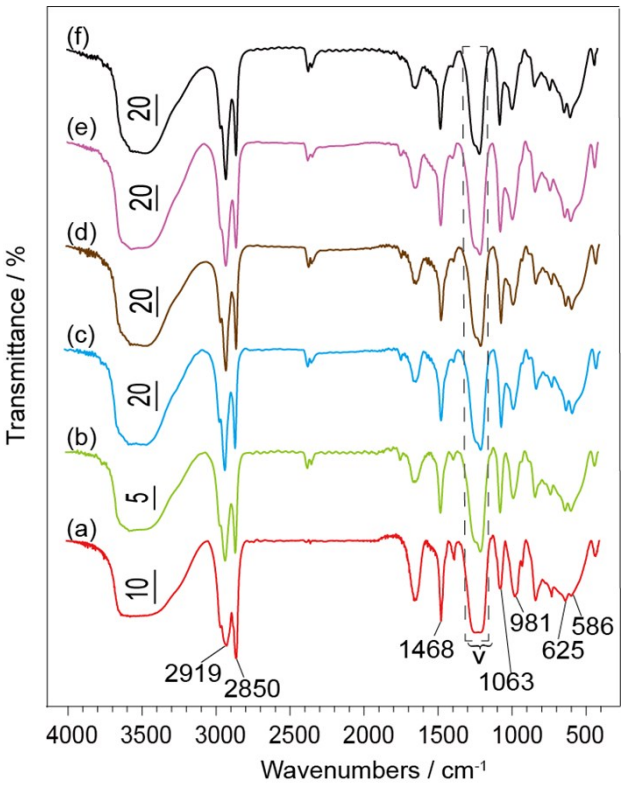

Fig. S6 FT-IR spectra for DS^{-}-$LEu_xTb_{1-x}Hs$ of (a) x = 0, (b) x = 0.05, (c) x = 0.2, (d) x = 0.5, (e) x = 0.8 and (f) x=0.95.

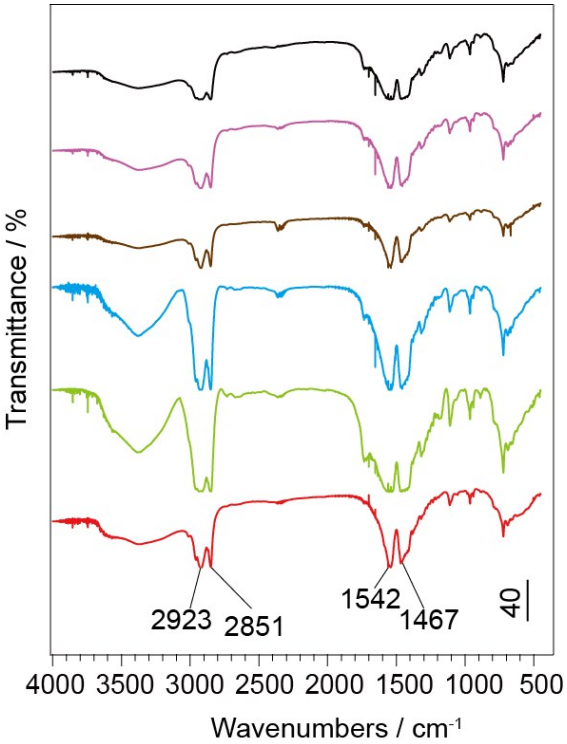

Fig. S7 FT-IR spectra for OA^{-}-$LEu_xTb_{1-x}Hs$ when (a) x = 0, (b) x = 0.05, (c) x = 0.2, (d) x = 0.5, (e) x = 0.8 and (f) x = 0.95.

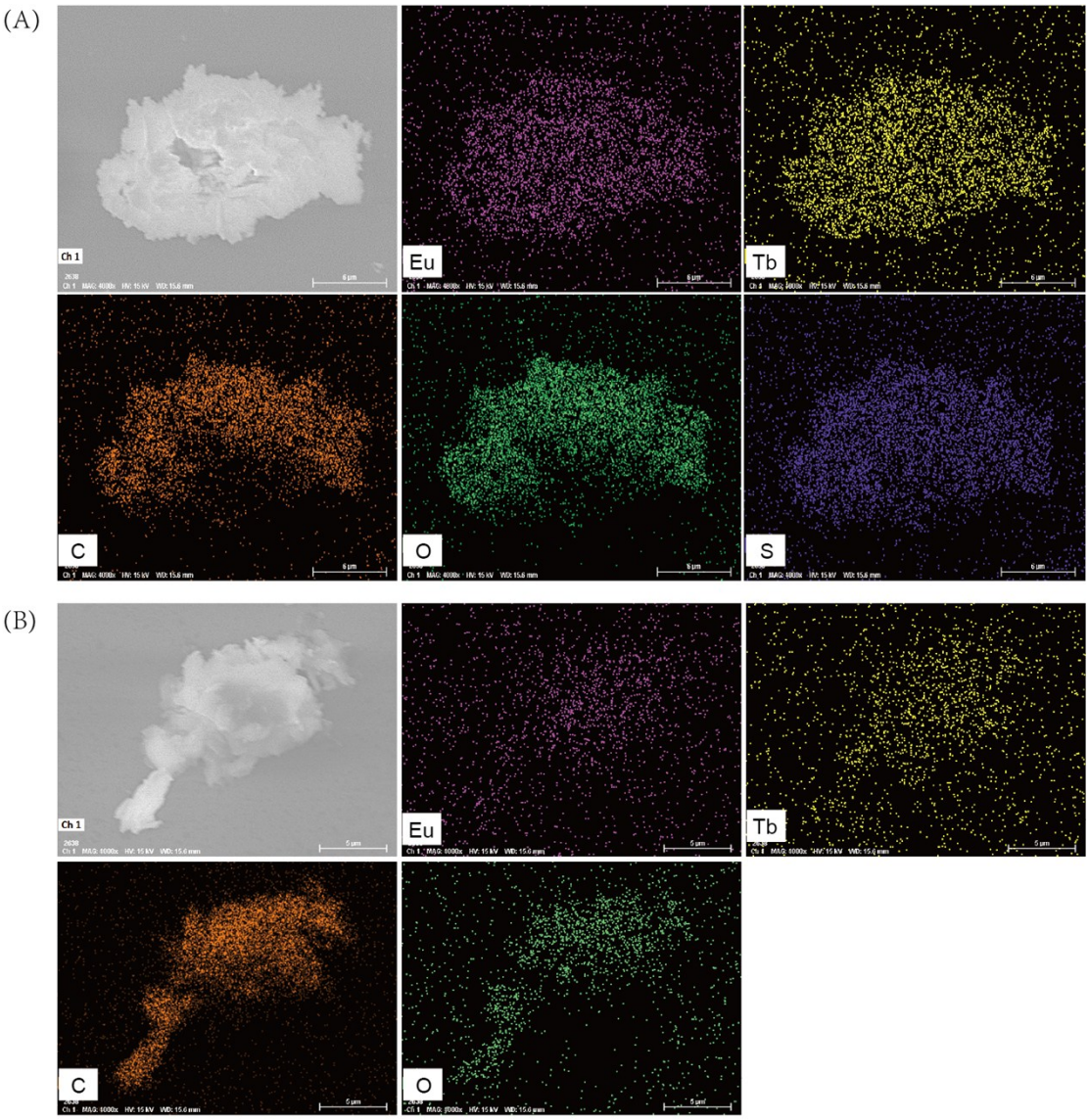

Fig. S8. SEM/EDX mapping images of (A) DS^-- and (B) OA^--$LEu_{0.5}Tb_{0.5}H$.

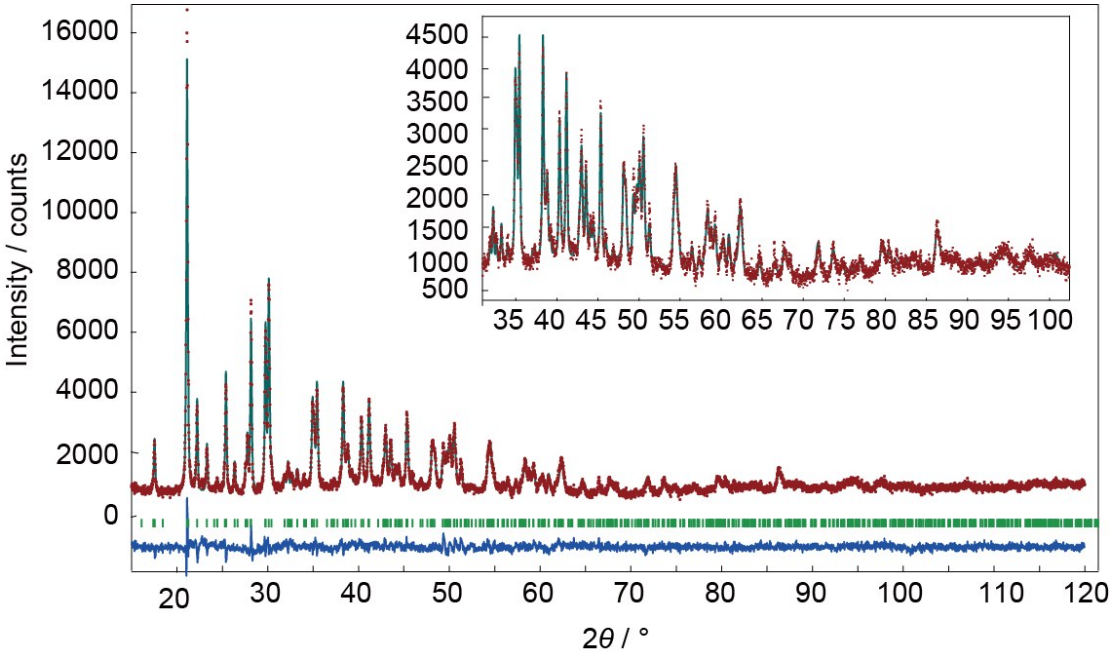

Fig. S9 Fitting patterns of EuTb-Tb8 for Cl^--$LEu_{0.5}Tb_{0.5}H$. The experimental and simulated intensity data are plotted as dotted and solid lines, respectively; the line at the bottom is their intensity difference.

Table S4 Structure parameters of EuTb-Tb8 for Cl^--$LEu_{0.5}Tb_{0.5}H$.

Atom	Wyckoff index	x	y	z	*g*	*B*/Å^2
Tb	4c	0.272(2)	0.254(1)	0.930(6)	1.0	0.746(5)
Eu(1)	2b	0	0.5	0.949(3)	1.0	0.746(5)
Eu(2)	2a	0	0	0.929(9)	1.0	0.746(5)
OH(1)	4c	0.486(1)	0.269(4)	0.905(3)	1.0	0.550(7)
OH(2)	4c	0.083(5)	0.225(1)	0.847(3)	1.0	0.550(7)
OH(3)	4c	0.164(8)	0.429(5)	0.088(2)	1.0	0.550(7)
OH(4)	4c	0.646(9)	0.431(8)	0.925(1)	1.0	0.550(7)
OH(5)	4c	0.140(1)	0.733(7)	0.829(9)	1.0	0.550(7)
H_2O(1)	4c	0.200(7)	0.801(3)	0.375(9)	1.0	3.394(7)
H_2O(2)	2b	0	0.5	0.627(6)	0.36	3.394(7)
H_2O(3)	2a	0	0	0.616(1)	0.54	3.394(7)

Cl	4c	0.125(7)	0.286(9)	0.430(8)	1.0	2.069(2)

Space group: $P2_12_12$ (no. 18); a = 12.872(3) Å; b = 7.298(0) Å; c = 8.438(0) Å; V = 792.6 (9) Å^3; R_{wp} = 7.301%, R_p = 5.712%, R_R = 19.326%, R_e = 2.834%, S = 2.577%.

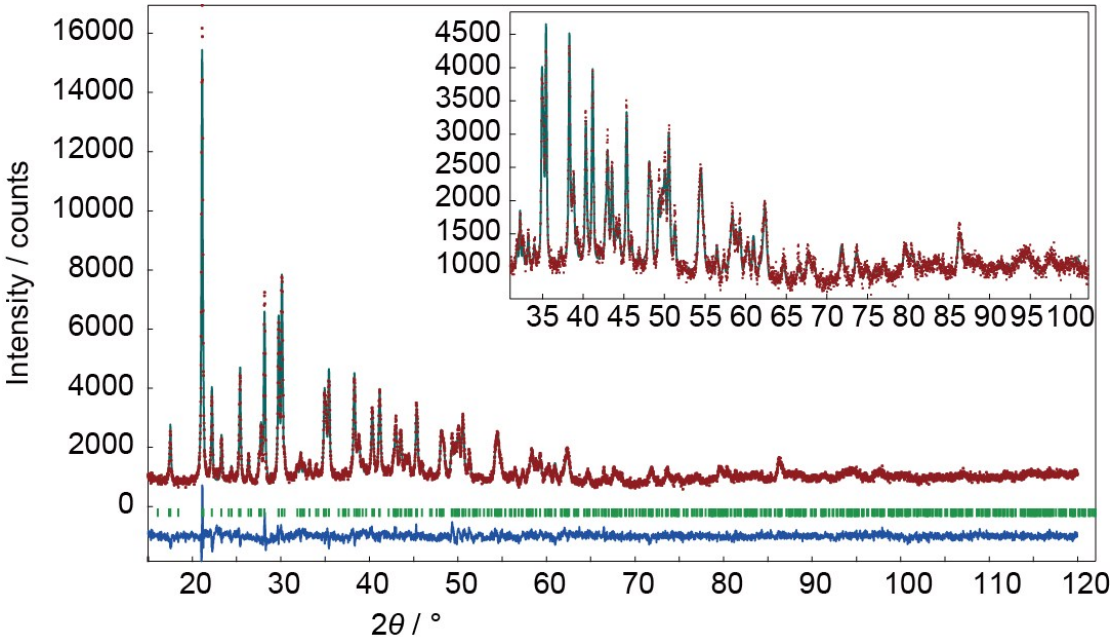

Fig. S10 Fitting patterns of EuTb-Tb9 of Cl^--$LEu_{0.5}Tb_{0.5}H$. The experimental and simulated intensity data are plotted as dotted and solid lines, respectively; the line at the bottom is their intensity difference.

Table S5 Structure parameters of EuTb-Tb9 for Cl^--$LEu_{0.5}Tb_{0.5}H$.

Atom	Wyckoff index	x	y	z	g	B/Å^2
Eu	4c	0.272(0)	0.249(9)	0.928(7)	1.0	0.929(1)
Tb(1)	2b	0	0.5	0.952(2)	1.0	0.929(1)
Tb(2)	2a	0	0	0.930(1)	1.0	0.929(1)
OH(1)	4c	0.485(2)	0.270(1)	0.904(3)	1.0	0.360(3)
OH(2)	4c	0.083(9)	0.243(0)	0.838(2)	1.0	0.360(3)
OH(3)	4c	0.165(9)	0.414(5)	0.088(4)	1.0	0.360(3)
OH(4)	4c	0.645(6)	0.443(3)	0.924(4)	1.0	0.360(3)

OH(5)	4c	0.145(8)	0.760(3)	0.834(7)	1.0	0.360(3)
$H_2O(1)$	4c	0.198(3)	0.821(9)	0.379(9)	1.0	3.129(7)
$H_2O(2)$	2b	0	0.5	0.606(7)	0.36	3.129(7)
$H_2O(3)$	2a	0	0	0.628(1)	0.54	3.129(7)
Cl	4c	0.125(2)	0.214(3)	0.428(2)	1.0	2.939(7)

Space group: $P2_12_12$ (no. 18); a = 12.863(8) Å; b = 7.292(8) Å; c = 8.431(7) Å; V = 791.0 (3) Å^3; R_{wp} = 7.395%, R_p = 5.788%, R_R = 19.859%, R_e = 2.839%, S = 2.604%.

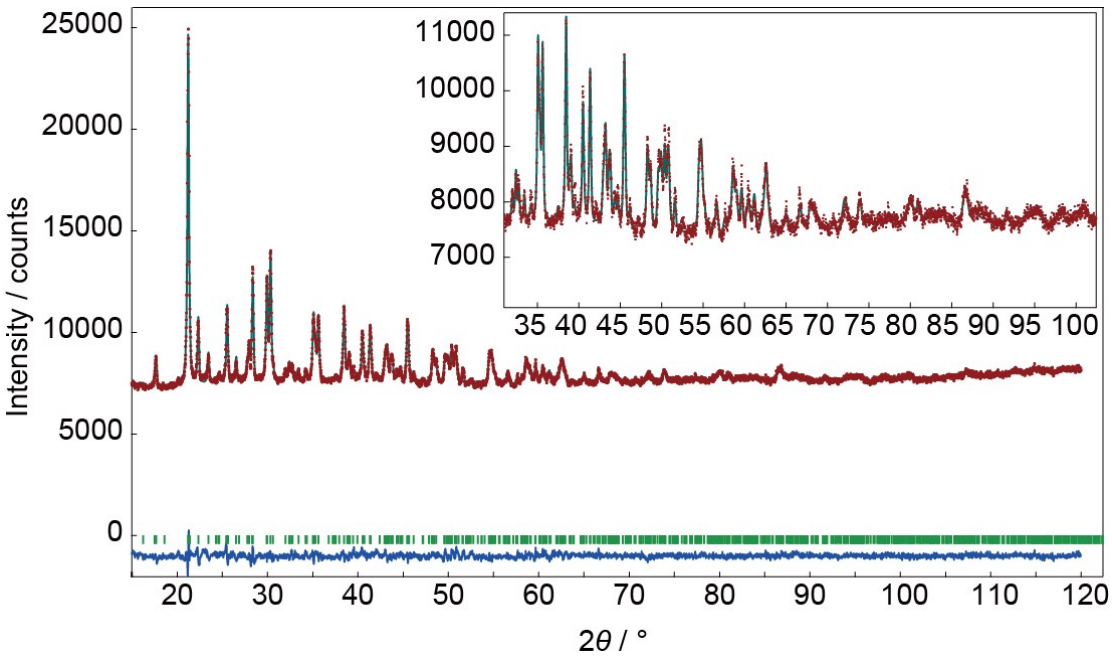

Fig. S11 Fitting patterns of Cl^--$LEu_{0.05}Tb_{0.95}H$. The experimental and simulated intensity data are plotted as dotted and solid lines, respectively; the line at the bottom is their intensity difference.

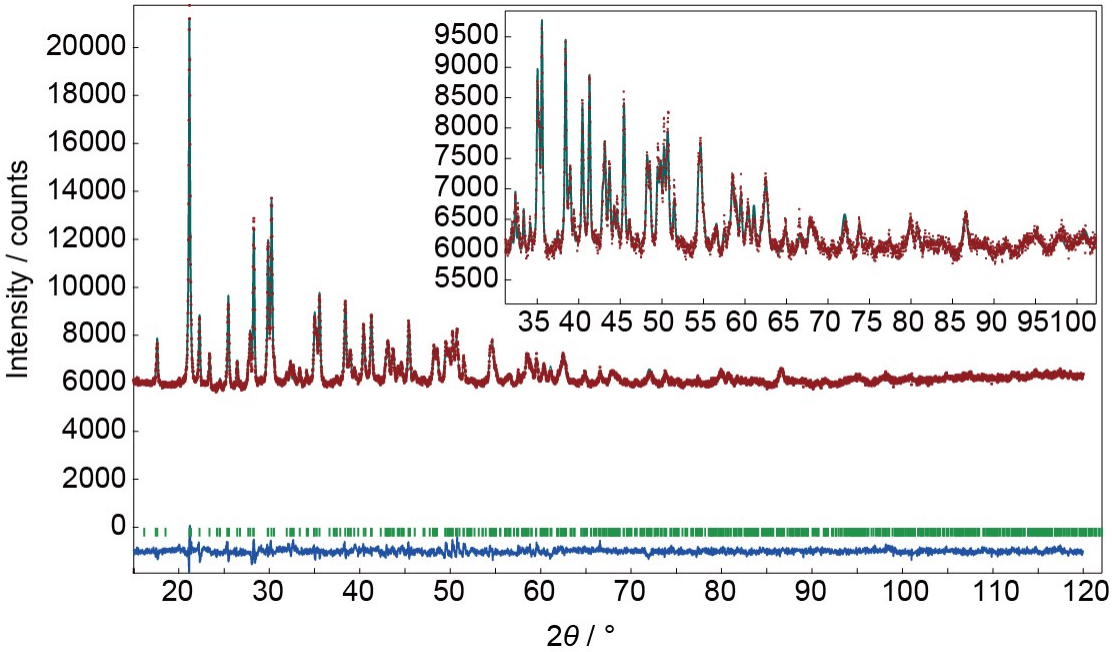

Fig. S12 Fitting patterns of Cl^--$LEu_{0.2}Tb_{0.8}H$. The experimental and simulated intensity data are plotted as dotted and solid lines, respectively; the line at the bottom is their intensity difference.

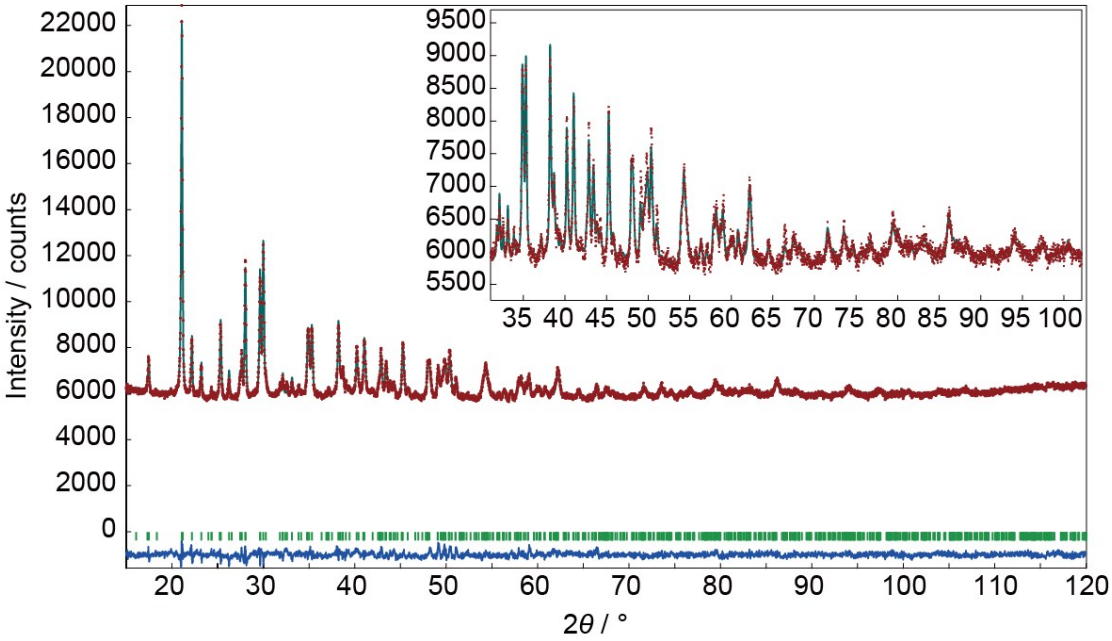

Fig. S13 Fitting patterns of Cl^--$LEu_{0.8}Tb_{0.2}H$. The experimental and simulated intensity data are plotted as dotted and solid lines, respectively; the line at the bottom is their intensity difference.

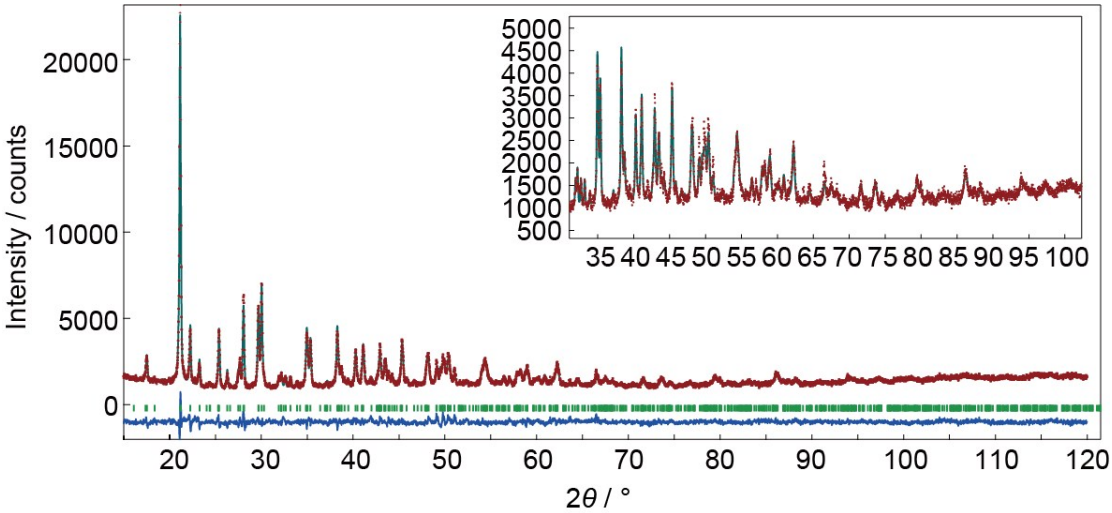

Fig. S14 Fitting patterns of Cl^--$LEu_{0.95}Tb_{0.05}H$. The experimental and simulated intensity data are plotted as dotted and solid lines, respectively; the line at the bottom is their intensity difference.

Table S6 Structure parameters of Cl^--$LEu_{0.05}Tb_{0.95}H$.

Atom	Wyckoff index	x	y	z	*g*	*B*/Å^2
T1	4c	0.271(2)	0.252(6)	0.928(6)	1.0	1.056(9)
T2	2b	0	0.5	0.952(2)	1.0	1.056(9)
T3	2a	0	0	0.929(5)	1.0	1.056(9)
OH(1)	4c	0.481(2)	0.265(4)	0.899(2)	1.0	0.901(1)
OH(2)	4c	0.061(7)	0.193(1)	0.904(4)	1.0	0.901(1)
OH(3)	4c	0.147(4)	0.442(0)	0.100(4)	1.0	0.901(1)
OH(4)	4c	0.641(5)	0.409(9)	0.924(0)	1.0	0.901(1)
OH(5)	4c	0.135(8)	0.744(9)	0.835(5)	1.0	0.901(1)
H_2O(1)	4c	0.200(0)	0.784(2)	0.365(2)	1.0	3.149(4)
H_2O(2)	2b	0	0.5	0.600(0)	0.36	3.149(4)
H_2O(3)	2a	0	0	0.611(9)	0.54	3.149(4)
Cl	4c	0.120(4)	0.280(7)	0.430(1)	1.0	1.341(5)

Space group: $P2_12_12$ (no. 18); a = 12.817(2) Å; b = 7.261(1) Å; c = 8.422(4) Å; V =783.8 (4) Å^3; R_{wp} = 1.320%, R_p =1.003%, R_R = 20.359%, R_e = 1.116%, S = 1.18%.

Table S7 Structure parameters of Cl^--$LEu_{0.2}Tb_{0.8}H$.

Atom	Wyckoff index	x	y	z	*g*	*B*/Å^2
T1	4c	0.271(4)	0.251(6)	0.932(2)	1.0	0.766(6)
T2	2b	0	0.5	0.949(9)	1.0	0.766(6)
T3	2a	0	0	0.929(5)	1.0	0.766(6)
OH(1)	4c	0.493(8)	0.291(1)	0.907(1)	1.0	0.796(3)
OH(2)	4c	0.085(7)	0.282(6)	0.851(8)	1.0	0.796(3)
OH(3)	4c	0.158(5)	0.443(5)	0.083(9)	1.0	0.796(3)
OH(4)	4c	0.647(2)	0.426(9)	0.927(5)	1.0	0.796(3)

OH(5)	4c	0.147(1)	0.728(0)	0.826(1)	1.0	0.796(3)
H_2O(1)	4c	0.219(8)	0.688(5)	0.372(2)	1.0	4.917(1)
H_2O(2)	2b	0	0.5	0.624(8)	0.36	4.917(1)
H_2O(3)	2a	0	0	0.608(5)	0.54	4.917(1)
Cl	4c	0.123(0)	0.299(6)	0.438(7)	1.0	0.803(6)

Space group: $P2_12_12$ (no. 18); a = 12.828(3) Å; b = 7.269(8) Å; c = 8.424(6) Å; V = 785.6 (3) Å^3; R_{wp} = 1.563%, R_p = 1.194%, R_R = 19.214%, R_e = 1.250%, S = 1.25%.

Table S8 Structure parameters of Cl^--$LEu_{0.8}Tb_{0.2}H$.

Atom	Wyckoff index	x	y	z	*g*	*B*/Å^2
T1	4c	0.270(8)	0.255(1)	0.926(2)	1.0	0.245(8)
T2	2b	0	0.5	0.948(2)	1.0	0.245(8)
T3	2a	0	0	0.931(6)	1.0	0.245(8)
OH(1)	4c	0.460(9)	0.250(0)	0.893(4)	1.0	0.285(4)
OH(2)	4c	0.048(2)	0.129(5)	0.974(5)	1.0	0.285(4)
OH(3)	4c	0.145(6)	0.434 (0)	0.075(6)	1.0	0.285(4)
OH(4)	4c	0.654(7)	0.424(0)	0.905(1)	1.0	0.285(4)
OH(5)	4c	0.139(7)	0.744(3)	0.835(3)	1.0	0.285(4)
H_2O(1)	4c	0.178(9)	0.724(9)	0.373(2)	1.0	1.534(9)
H_2O(2)	2b	0	0.5	0.509(3)	0.36	1.534(9)
H_2O(3)	2a	0	0	0.623(2)	0.54	1.534(9)
Cl	4c	0.113(6)	0.308(2)	0.432(1)	1.0	1.035(1)

Space group: $P2_12_12$ (no. 18); a = 12.931(6) Å; b = 7.333(0) Å; c = 8.450(8) Å; V = 801.3 (6) Å^3; R_{wp} = 1.512%, R_p = 1.161%, R_R = 120.777%, R_e = 1.263%, S = 1.19%.

Table S9 Structure parameters of Cl^--$LEu_{0.95}Tb_{0.05}H$.

Atom	Wyckoff index	x	y	z	g	B/Å^2
T1	4c	0.270(7)	0.254(5)	0.927(5)	1.0	0.822(4)
T2	2b	0	0.5	0.947(4)	1.0	0.822(4)
T3	2a	0	0	0.931(0)	1.0	0.822(4)
OH(1)	4c	0.468(0)	0.263(6)	0.901(4)	1.0	0.498(2)
OH(2)	4c	0.071(5)	0.167(4)	0.944(3)	1.0	0.498(2)
OH(3)	4c	0.145(5)	0.402(6)	0.084(5)	1.0	0.498(2)
OH(4)	4c	0.652(8)	0.441(1)	0.916(0)	1.0	0.498(2)
OH(5)	4c	0.131(2)	0.739(4)	0.857(0)	1.0	0.498(2)
H_2O(1)	4c	0.182(0)	0.771(5)	0.383(9)	1.0	1.572(5)
H_2O(2)	2b	0	0.5	0.627(2)	0.36	1.572(5)
H_2O(3)	2a	0	0	0.626(9)	0.54	1.572(5)
Cl	4c	0.117(0)	0.299(8)	0.435(1)	1.0	1.423(4)

Space group: $P2_12_12$ (no. 18); a = 12.935(1) Å; b = 7.336(0) Å; c = 8.439(6) Å; V = 800.8 (5) Å^3; R_{wp} = 6.162%, R_p = 4.795%, R_R = 21.478%, R_e = 2.545%, S = 2.42%.

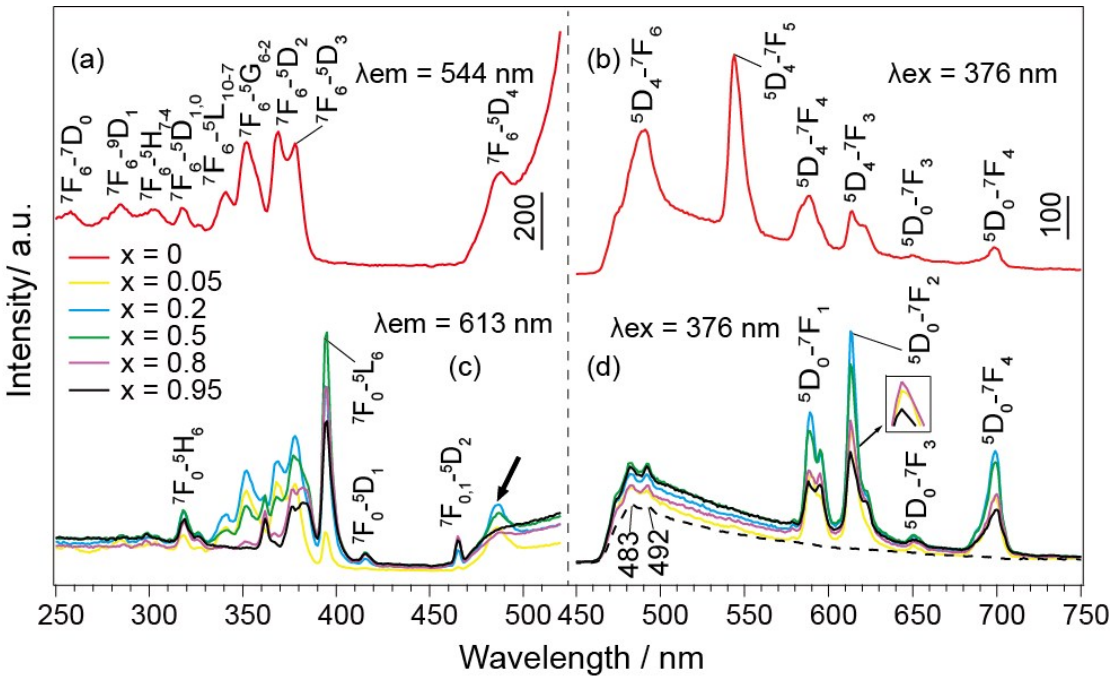

Fig. S15 (a, c) Excitation and (b, d) emission spectra of DS$^-$-LEu$_x$Tb$_{1-x}$Hs. The peaks at 483 and 492 nm (dashed line) are due to spectral responses of the equipment by the blank test.

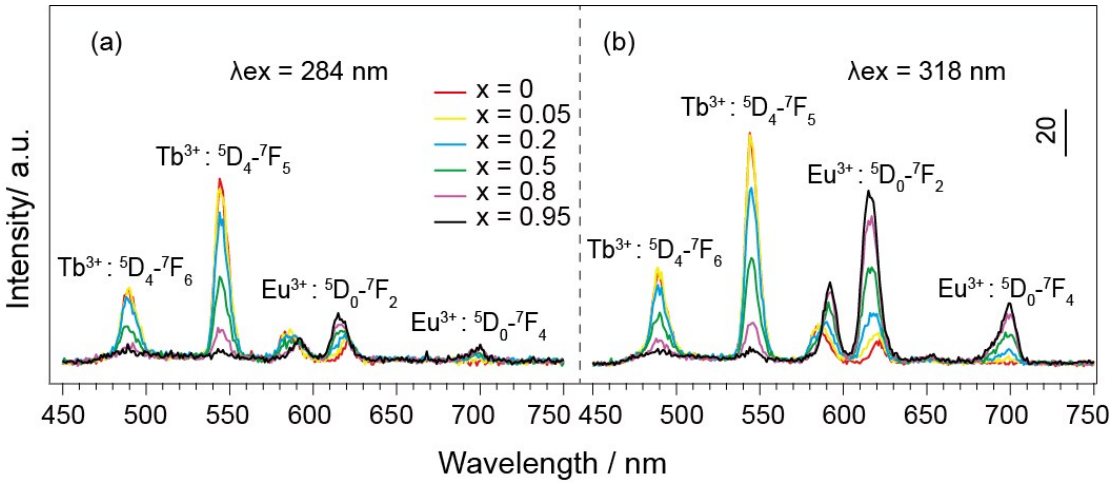

Fig. S16 Emission spectra of NSs-LEu$_x$Tb$_{1-x}$Hs excited at 284 and 318 nm.